Design and implementation of a novel contact resistivity measurement method for solar Si-ZnO:Al contacts.

Bart van Pelt

May 13, 2022

Abstract

TODO: lipsum vervangen

Lorem ipsum dolor sit amet, consectetuer adipiscing elit. Ut purus elit, vestibulum ut, placerat ac, adipiscing vitae, felis. Curabitur dictum gravida mauris. Nam arcu libero, nonummy eget, consectetuer id, vulputate a, magna. Donec vehicula augue eu neque. Pellentesque habitant morbi tristique senectus et netus et malesuada fames ac turpis egestas. Mauris ut leo. Cras viverra metus rhoncus sem. Nulla et lectus vestibulum urna fringilla ultrices. Phasellus eu tellus sit amet tortor gravida placerat. Integer sapien est, iaculis in, pretium quis, viverra ac, nunc. Praesent eget sem vel leo ultrices bibendum. Aenean faucibus. Morbi dolor nulla, malesuada eu, pulvinar at, mollis ac, nulla. Curabitur auctor semper nulla. Donec varius orci eget risus. Duis nibh mi, congue eu, accumsan eleifend, sagittis quis, diam. Duis eget orci sit amet orci dignissim rutrum.

Nam dui ligula, fringilla a, euismod sodales, sollicitudin vel, wisi. Morbi auctor lorem non justo. Nam lacus libero, pretium at, lobortis vitae, ultricies et, tellus. Donec aliquet, tortor sed accumsan bibendum, erat ligula aliquet magna, vitae ornare odio metus a mi. Morbi ac orci et nisl hendrerit mollis. Suspendisse ut massa. Cras nec ante. Pellentesque a nulla. Cum sociis natoque penatibus et magnis dis parturient montes, nascetur ridiculus mus. Aliquam tincidunt urna. Nulla ullamcorper vestibulum turpis. Pellentesque cursus luctus mauris.

Contents

Introduction

Motivatie Wat is ZnO:Al, en waarom is het interessant voor zonnecellen?

- **Bepaalde goede eigenschappen** Uniek als passiverende TCO.
- **Wat betekenen deze eigenschappen?** Wordt uitgelegd in deel I.

Wat moet er nog gebeuren? Nog weinig bekend over contactweerstand -> onderwerp van deze thesis.

Wat wil ik hier over leren? Hoe hangt de contactweerstand af van doping (Si, ZnO:Al) en anneal?

- **Bijvraag** Is het mogelijk om een goede contactweerstand te krijgen *tegelijkertijd* met goede conductiviteit en transparantie?
- **Hamvraag** Goed genoeg voor efficiënte zonnecellen?

Hoe ga ik dat doen? ALD ZnO:Al op verschillende substraten deponeren en annealen, dan doormeten.

- **Wat zijn de resultaten?** Wordt besproken in deel I.
- **Caveat: hoe ga ik dit doormeten?** Bleek verrassend lastig, methode verbeterd, zie deel II.

QUESTION: Ik wil Percspective ergens noemen, is dit een goede plek?

Part I

Figures

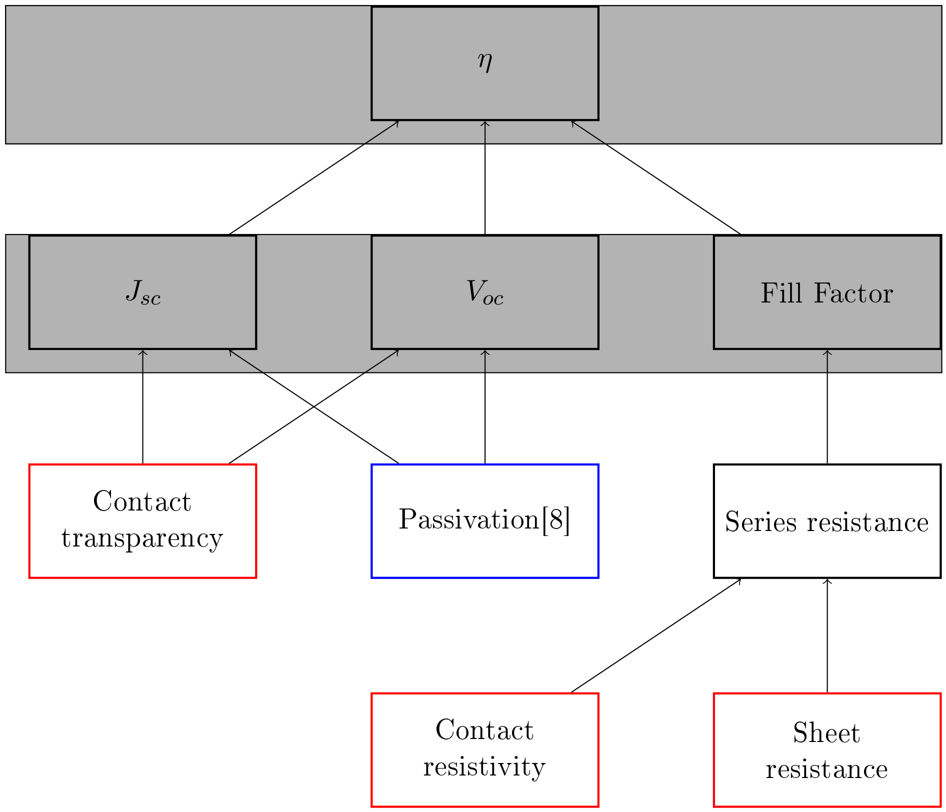
η
J_{sc}
V_{oc}
Fill Factor
Contact transparency
Passivation[8]
Series resistance
Contact resistivity
Sheet resistance

Part II

Zinc oxide contacts for solar cells

Chapter 1

Content

TODO: eerst verhaal uitwerken, dan pas opdelen in background, intro, etc...

Zonnecellen zijn belangrijk voor de energietransitie Mogen efficiënter want BOS kosten domineren.

Tevens schaarste Indium Nieuwe contactmaterialen nodig.

AZO lijkt een goede kandidaat Want transparant, geleidt goed, veelvoorkomend, en passiveert (uniek in dit opzicht).

Wat voeg ik hier aan toe? Contactgedrag op silicium, onderwerp van deze thesis.

Formulering doel Goede zonnecellen met passiverende AZO contacten.

Definieer "goede zonnecel" Welke zonnecelparameters zijn belangrijk? **Background** Ook belangrijk: kwantificeer, wat is laag genoeg qua serieweerstand?

J_{sc} Wordt beinvloed door passivatie en transparantie.

V_{oc} Ook recombinatie.

Serieweerstand Onderwerp deze thesis, liefst zo laag mogelijk, specifieker: contactweerstand.

Definieer "goed contact" contact is losjes gedefinieerd als totale contact stack, dus inclusief passivatie.

Goede laterale geleiding Transport naar metalen grid. Al bekend, haalbaar voor AZO. Belangrijk voor serieweerstand.

Goede transparantie Anders daalt efficiëntie via J_{sc}. Haalbaar Belangrijk voor J_{sc}.

Passivatie Onderdrukking recombinatie is cruciaal voor efficiëntie. Ook haalbaar. SOURCE: Bas Belangrijk voor J_{sc}.

Goede interface geleiding Mijn onderwerp, belangrijk voor serieweerstand.

Welke procesparameters kunnen we beïnvloeden? Oftewel, waar ga ik mee experimenteren, en wat is hier al over bekend?

Capping met AlOx Cruciaal voor passivatie, SOURCE: Bas.

AZO doping Belangrijk voor geleidbaarheid AZO, wel slecht voor transparantie SOURCE: Dennis/ik. Ook goed voor passivatie SOURCE: Bas (door veldeffect, dit later noemen?)

Annealing Belangrijk voor passivatie.

Si doping Belangrijk voor lage contactweerstand SOURCE: Schroder, wel slecht voor Auger recombinatie.

Vraag Kunnen we met AZO/Si contacten maken die goed passiveren, goed lateraal geleiden, transparant zijn, *en* een lage contactweerstand hebben?

Plan van aanpak AZO doping, annealing, en Si doping variëren. In plane eigenschappen checken met Hall, optisch met SE, en contactweerstand met nieuwe methode.

Stresspunt eigen bijdrage Dit blijkt niet triviaal, nieuwe contactweerstandmethode en selectieve AlOx ets bleken nodig, hier ontwikkeld.

Hoe ga ik dit doen? Sample processing Eerst twee types sample beschrijven.

ALD Supercycles, reactor, recepten, etc..

Anneal Methodiek, hotplate tot 500C, daarboven RTA.

Voor contactweerstand Ets + Ag

Etsproces Wordt later geverificeerd, welke stoffen, welke temperatuur, hoe lang bleek sufficient?

Ag evap e-beam evaporation, details beschrijven

Karakterisatie Welke meetmethodes gebruik ik?

Hall Conductiviteit: Mobiliteit, carrier density, soortelijke weerstand.

SE Transparantie: Free carrier absorption, tevens info over mobiliteit, effectieve massa en AZO bandgap.

Ook gebruikt voor laagdiktes belangrijk voor testen etsproces.

Contactweerstandsmethode Contactweerstand (duh!)

Wat kan ik met de data? Framing: hoe maak je "goede" contacten? (Dit wordt ongeveer resultaten/discussie)

Eerst opstapje Waarom deze parameters gebruikt voor contactweerstandmetingen? Niet te veel detail, stukjes terugpakken. Dit stuk overlapt voor een groot deel met Dennis, ik focus hier op de lessen qua procesparameters zodat ik verder kan naar contactweerstanden. Voor meer details over de onderliggende fysica: zie thesis Dennis.

Capping Duidelijk cruciaal voor geleidbaarheid (Hall). Ook al eerder gevonden, niet teveel tijd aan kwijt raken. Plotje sheet resistance vs anneal -> Capping cruciaal.

Doping Belangrijk voor geleidbaarheid AZO, wel slecht voor transparantie (samenvatten met J_{sc} grafiek.) Dus: lage dotering gebruiken, sufficient voor geleidbaarheid.

Anneal 500C beste voor passivatie (al gepubliceerd). Hierboven stijgt tevens carrier density.

Intermezzo Okay, nu willen we door naar contactweerstanden, maar dan moeten we wel kunnen etsen. QUESTION: is dit hier een goede plek voor?

Ets data Laat zien dat de dikte van AlOx sterk afneemt, terwijl de fitdikte van ZnO constant blijft. Data is wat ruw voor langere etstijden, ook niet helemaal duidelijk in welke mate iets roughness of ZnO is, maar initiele slope geeft aan dat een ets van een paar minuten prima zou moeten zijn om AlOx te verwijderen.

Contactweerstand Wat doen deze parameters nu voor de contactweerstand?

Anneal Bij iZnO verlaging, verder verhoging. Mogelijk door verplaatsing Al dopants, dit effect speelt niet in iZnO.

AZO doping Gedoteerd heeft lagere weerstand dan intrinsiek. Mogelijk Burstein-Moss shift

Opvallend Op 260nplus geeft r48 een hogere weerstand dan r96. Mogelijk door afstand eerste doping plane tot interface. QUESTION: Maar waarom dan niet op 130nplus?

Si doping Verlaagt contactweerstand. Schottky model, van toepassing op accumulatiecontact?

Overall Lage contactweerstand goed haalbaar en compatible met passivatie/TCO

Conclusie AZO lijkt ook qua contactweerstand erg geschikt voor zonnecellen.

Chapter 2

Introduction

Chapter 3

Background

3.1 Solar cell parameters

Loosely framed the goal of this work is to find out if ZnO:Alpassivating contacts can make *good* solar cells. To start answering this question, let's first narrow down what is meant by a *good* solar cell, before diving into the details about contacting layers. The purpose of solar cells is clear: to convert thermal radiation into usable electrical energy. In the ideal case, the incoming thermal power, P_{in}, is totally converted to electrochemical power, $V_{\mathrm{out}}I_{\mathrm{out}}$, of course this total conversion is thermodynamically forbidden, the best we can do is to maximize the efficiency,

$$\eta = \frac{V_{\mathrm{out}}I_{\mathrm{out}}}{P_{\mathrm{in}}}. \tag{3.1}$$

Since we cannot control the power output of the sun, this task practically boils down to maximizing the $V_{\mathrm{out}}I_{\mathrm{out}}$ product. Two useful parameters of this current-voltage characteristic are the short circuit current, J_{sc}, and the open circuit voltage, V_{oc}. As the output current depends on the output voltage, these two limiting cases are not enough to know the cells efficiency, so a third parameter, the fill factor (FF) is introduced. Ideally, a solar cell would sustain full current output without a decline in output voltage, operating at an output power $V_{\mathrm{out}}I_{\mathrm{out}}$. Realistically though, there is some optimal operating voltage, V_{MP}, at which the cell produces its maximal power, delivering a current I_{MP}. This ratio of *real* output power and *ideal* output power is what defines the fill factor:

$$\mathrm{FF} = \frac{I_{\mathrm{MP}}V_{\mathrm{MP}}}{I_{\mathrm{sc}}V_{\mathrm{oc}}}. \tag{3.2}$$

TODO: plotje IV karakteristiek + FF In terms of these cell parameters, the efficiency can then be expressed as

$$\eta = \frac{I_{\mathrm{sc}} V_{\mathrm{oc}} \mathrm{FF}}{P_{\mathrm{in}}}. \tag{3.3}$$

Measuring these cell parameters requires the fabrication of complete cells, to optimize a ZnO:Al contact we should shift our focus to directly measurable material properties. Among the desired qualities of a contact are a high transparency, good passivation and a low series resistance. Let's take a look at how these parameters influence the overall solar cell performance.

A typical high school explanation of solar cells goes as follows:

1. A photon from the sun is absorbed by the solar cell, here it rips an electron apart from an atom in the crystal, transferring its energy. The electron is negatively charged, but the void it leaves effectively has an opposite charge of equal magnitude, this void is called a "hole".

2. The electron finds its way to one contact of the solar cell, while the hole finds its way to the other.

3. The electron *really* wants to get back to the hole, and the easiest way to do so is to go through the device that you want to power. The electrical energy from the electron is then transferred to the device, providing useful energy.

This rudimentary explanation completely skims over the complex thermodynamical nature of this energy conversion. Moreover it fails to answer basic questions such as "but why do the electrons and holes move away from each other if they attract each other?" and "okay, so the charges made it to the contacts, why would they not just go back the way they got there instead of taking the whole wire/device detour?". Despite these and several more shortcomings, this simple model can give us some meaningful heuristic insights into what is needed to make a good front contact. Let's go through the explanation again, and see what can go wrong with each step.

1. A photons should transfer its energy to an electon-hole pair, what if it can't? This can occur due to several reasons.

   (a) The photon does not have enough energy to create an electron-hole pair in the base; that is, the photon has an energy below the so-called bandgap of the solar cell's base.

(b) The photon does transfer all of its energy to an electron-hole pair, but the electron-hole pair loses some energy afterwards. This process is called thermalization, by collisions with the crystal atoms the electrons and holes lose energy until they get stuck at an energy similar to the bandgap.

(c) The photon might not even get to the base of the solar cell. If the photon is absorbed in the front contact or reflected by the metal interconnections, its energy is effectively lost. For this reason the front contact should obviously be as transparent as possible.

(d) The photon is reflected. If a solar cell reflects a photon back towards the sky, the photon's energy will not be of much use. A few strategies are used to keep photons trapped in a cell, texturing and antireflection coatings. While light trapping is very important for solar cell efficiency, it will not be further discussed in this thesis.

2. Maybe the electron and hole don't make it to their intended contacts.

   (a) An electron or hole could reach the wrong contact. In the high-school explanation this sounds very likely, after all, the positive holes should be strongly attracted to the contact that's filled with negative electrons (and vice versa), right?

   A crucial part to this selectivity is that the contacts should be highly conductive to one type of carrier, while highly resistive to the other. Thus, for n-type contacts a very low electron resistivity should be obtained. A more in-depth discussion of selectivity will be given in TODO: waar? .

   (b) What if the electron and hole don't even make it to the contacts? It's possible for the newly formed electron and hole to recombine with each other (or with other electrons and holes), if this happens their electrochemical energy will be lost (of course energy is conserved, but from an engineering perspective it will probably not be useful energy anymore). One possible mechanism for this is radiative recombination, in which an electron and hole form a photon. Luckily, this rarely occurs in crystalline silicon due to its indirect bandgap, which means that some additional momentum is needed for this reaction to occur. In crystalling silicon, the most significant recombination pathways are Shockley-Read-Hall (SRH) and Auger recombination. In the former pathway electrons can make small jumps in energy using crystal imperfections, these small jumps are more likely to occur than a single large jump. The latter uses a third electron or hole to absorb the excess momentum that makes a direct transition improbable. Suppressing recombination is very important for efficient solar cells, and it is referred to as passivation.

3. Maybe the generated charges do not transfer their energy to the intended load. This can happen if a parasitic series resistance is present in the circuit, as these create potential gradients. In these gradients the electrons lose some useful energy, which cannot be used in the device. For this reason all parasitic series resistances should be minimized. This series resistance can be attributed to a few contributions. First, the carriers need to experience a low resistance during transport from the cell bulk to the contact, this is called contact resistivity. Second, once in the contact the carriers should freely flow towards the metal connections, for this a low in-plane resistance is required.

With this oversimplified treatment of solar cell physics, it already becomes clear that highly transparent highly conductive contacting layers are essential for efficient solar cells, moreover, a high degree of passivation should be achieved so that the generated free charge carriers do not recombine.

ZnO:Al is a material that has gained attention for being highly transparent and conductive, at the same time it offers passivation on c-Si, giving it a unique combination of properties. Previous work has shown that a good passivation can be achieved by hydrogenation of surface defects by annealing the material while it is covered with an Al_2O_3 capping layer SOURCE: todo . This combination of capping and annealing has been previously studied within the PMP group, resulting in a publication that includes parts of this work SOURCE: paper . There (and in this work), the presence of a capping layer was found to be critical for achieving a high in-plane ZnO:Al conductivity and transparency. An important remaining piece of the puzzle is then to find out whether a low contact resistivity can be achieved as well, this is the focus of this work.

To do this turned out not to be an easy task, put shortly: measuring contact resistances of ZnO:Al is difficult to do by conventional methods which often require patterning and etching to create sample structures. Furthermore, the presence of the Al_2O_3 capping layer makes it impossible to directly contact the ZnO:Al film of interest (at least for contact resistivity measurements).

Due to these metrological difficulties a new measurement method was designed and implemented, which is discussed in detail in the second part of this thesis.

For the first part of this thesis, let's dive into the really interesting question: does ZnO:Al make good solar cell contacts?

As a start we'll rid ourselves of the thusfar handwavy (and dramatically oversimplified) solar cell description so that questions can be framed quantitatively, so far it's only become clear that the contact resistivity should be low, but how is it even defined, and what is low enough? Then the experimental methodology will be discussed, including sample preparation, process parameters of interest, and measurement methods. Following will be an outline of experimental work on in-plane resistance and transparency, and how different process parameters influence these. This part of the work was done in partial collaboration with Dennis Loeffen, who discussed these fully in his masters' thesis SOURCE: Dennis , here these results are treated with less detail, focussing on what these results can tell us about which process conditions are needed to obtain low transparencies and low in-plane resistances. Finally, it will be shown that ZnO:Al contacts can have a promisingly low contact resistivity on c-Si, moreover, this can be achieved in a process window in which the other relevant material properties are also excellent.

3.2 Contact resistivity: why relevant

In this section TODO: or chapter? , we will look into solar cell physics in some more detail. For a better understanding, a thermodynamic description of charge carriers in a semiconductor is needed. Semiconductors are defined by having a bandgap, a band of energy values for which no electron state exists. An electron is then either moving around in the conduction band, or bound to an atom while in the valence band. To move between the bands, energy needs to either be supplied to an electron in the valence band, or an electron in the conduction band needs to somehow get rid of a considerable amount of energy. These generation and recombination processes don't happen instantly, which enables electrons to stay in the conduction band for quite long times. The states within the valence band without an electron are called holes and they can be seen as carrying a positive charge, essentially due to the *absence* of an electron. This property is what distinguishes semiconductors from metals, in which no bandgap exists, in metals electrons are always free to decay into available lower energy states. For nondegenerate semiconductors the densities of electrons, n, and holes,

p, can be well described by Boltzmann statistics:

$$n = n_{\mathrm{CB}} \exp\left(-\frac{E_{\mathrm{CB}} - E_{\mathrm{F}_n}}{k_B T}\right); \tag{3.4}$$

$$p = n_{\mathrm{VB}} \exp\left(-\frac{E_{\mathrm{F}_p} - E_{\mathrm{VB}}}{k_B T}\right). \tag{3.5}$$

Here n_{CB} and n_{VB} are the densities of states in respectively the conduction and valence bands, E_{CB} and E_{VB} are the energy bounds of the conduction and valence bands, and E_{F_n} and E_{F_p} are the so called Fermi levels of the electron and hole ensembles. For thermal equilibrium it can readily be derived that $E_{\mathrm{F}_n} = E_{\mathrm{F}_p}$, but this changes when electron-hole pairs are actively generated. In this non-equilibrium situation, one can ask if Boltzmann statistics can be applied, after all, this is a result in equilibrium thermodynamics. Luckily, it typically takes picoseconds for electrons (or holes) to reach equilibrium among themselves, meanwhile, the equilibration between conduction and valence bands is much slower, electrons can take up to milliseconds on average to make the transition. This means that electrons can be considered in equilibrium, and so can holes, just not in equilibrium with each other. The excesses in electron and hole densities can be described by an increase in E_{F_n} and a decrease in E_{F_p}, a phenomenon called Fermi level splitting.

Due to the absence of a bandgap, the separate equilibration of electrons and holes does not occur in metals, furthermore thermal equilibration is a very fast process. This implies that, in a metal, the carrier statistics can be described by a single Fermi level: $E_{\mathrm{F}} = E_{\mathrm{F}_n} = E_{\mathrm{F}_p}$.

So far, the Fermi levels have been interpreted merely as a useful way to parametrize the carrier distributions, but they carry greater physical relevance. A more physical interpretation of the Fermi levels is that they correspond, up to sign, to the electrochemical potentials of both carriers, i.e. $E_{\mathrm{F}_n} = \eta_n$, $E_{\mathrm{F}_p} = -\eta_p$. The free energy of an electron-hole pair, which we want to extract, is then given by $E_{\mathrm{F}_n} - E_{\mathrm{F}_p}$. This picture also gives a more quantitative description of the heuristic "electrons want to move from one side of the cell to the other, transferring energy to the device". As the carrier statistics are described by only a single Fermi level in the contacts, the goal is to have a Fermi level difference between the two contacts, this potential difference can then be used to drive a current through a device.

This enables us to relate electron and hole currents to gradients in Fermi levels:

$$J_n = \frac{\sigma_n}{e} \nabla E_{\mathrm{F}_n}, \tag{3.6}$$

$$J_p = \frac{\sigma_p}{e} \nabla E_{\mathrm{F}_p}, \tag{3.7}$$

where $\sigma_n = en\mu_n$ and $\sigma_p = ep\mu_p$ are the conductivities of electrons and holes respectively, expressed in terms of the elementary charge and density and mobility of the specific carriers.

This statement corresponds to E_{F_n} being higher on one side of the cell than E_{F_p} on the other, the question is then how this can be realized. As noted before, metals do not exhibit Fermi level splitting, this means that while the Fermi levels are split in the bulk of the cell, they need to bend towards each other at the contacts. To get the desired asymmetry at a contact, one of the Fermi levels needs to bend strongly while the other does not. This can be achieved by controlling the conductivities to both carriers, an n-type contact should be very conductive to electrons, but very resistive to holes. This combination results in a strong gradient in E_{F_p}, and a nearly constant E_{F_n}. As the conductivities scale with carrier density, the most straightforward way to achieve this asymmetry is to strongly dope the contact, resulting in a very high electron density and a very low hole density. An additional benefit to this doping is that it reduces surface recombination at the contact interface, as thermal diffusion of holes always occurs, reducing the number of holes available to recombine can greatly improve passivation. Some care needs to be taken with this doping however, as an overabundance of free carriers can lead to the three-particle Auger recombination process and photon absorption in the contact, in practice a balance should be found between too little and too much doping. While the selectivity

- Selectivity
  - Combination with low J0 SOURCE: todo Regenboogplotje
  - Les: we hebben J0 laag (toch?) dus
- Tot zover: boel factoren besproken, ga ik niet te ver op in Wel recap, transparantie is belangrijk
- Hier even uitlichten: contactweerstand, waarom zo belangrijk?
  - Selectiviteit
  - Ohmic losses Back of envelope berekening

3.3 Methodiek

1. Preparatie recept etc

(a) Type 1

(b) Type 2

i. Ets

2. Metingen verwijs naar deel 2. Black boxes.

   (a) SE Model, plotje absorptiecoeffient vs w_t w_p

3.4 Results/discussion

Parameter space prunen. Ook passivatie meepakken.

- paper Bas
- Wel/niet tunneloxide.

Contactweerstanden.

3.5 Conclusie

Doping nodig, welke procesparameters. In principe groen licht voor AZO zonnecellen. Realiseren.

3.6 TODO todos

1. **TODO** Plaatjes in verhaal
2. **TODO** Additional insights?

Chapter 4

Theory

4.1 Solar cell operation

Globaal Hoe werkt een zonnecel? [8]

Doel Welke factoren bepalen efficiëntie?

Specifiek Welke impact heeft contactweerstand? Mooie plek voor het efficientie vs J_sc en ρ_c plotje, dan kan ik meteen bespreken waarom ook passivatie en transparantie zo belangrijk zijn.

4.2 Physics of semiconductor contacts

Achtergrond Zojuist besproken dat een lage contactweerstand en goede passivatie belangrijk zijn voor de hele cel, in deze sectie gaan we inzoomen op het contact zelf.

Vraag Hoe werken halfgeleider contacten, welke zaken zijn relevant voor dit werk?

Passivatiemechanismes Chemische passivatie vs veldpassivatie QUESTION: In principe heb il

::

4.3 ALD

QUESTION: Hele sectie waard? of bij methods even het recept goed beschrijven.

Chapter 5

Methods

Chapter 6

Results/discussion

Chapter 7

Conclusion

Part III

Contact resistivity measurements

Chapter 8

Introduction

In the previous part of this thesis, the contact resistivity of Al-doped zinc-oxide on doped silicon was investigated, while omitting details on the performed measurements. In this part of this thesis, the devised measurement setup and method will be described in full detail. The method provides an alternative to typical contact resistivity measurements, in which several processing steps are needed to create accurately shaped contacts on the samples of interest. These methods include the Cox and Strack (C&S) and Transfer Length Method (TLM) methods, which will be explained later. Not only are these steps time-consuming and complicated to perform, they pose limitations on the types of samples that can be used. Furthermore, thermal and chemical processing steps could alter the electrical properties of the contact of interest, and there is no guarantee that the tested contacts accurately resemble the contact as it would behave in a practical device. At the start of this project a simple measurement method was suggested, coat a sample with a thin film of silver, drive a current between the top and bottom of this sample and measure the resulting potential difference. Multiplying the obtained resistance by the area of the sample should then give the specific resistance of the sample. While this suggested pin-to-plate measurement is very easy to perform, not needing any patterning and etching steps as required by C&S and TLM, it quickly became clear that the method was so unreliable that useful data could not be obtained. As the C&S and TLM methods provide some significant challenges, the choice was made to look deeper into the pin-to-plate method, and see if it can be improved on enough to be useful. This work presents a solution to this problem, in which custom printed circuit boards are used to control the current flow in the samples. TODO: fill in this part The method devised here is able to characterize samples without the need of these patterning steps, requiring only a metallization step to ensure good contacts between the probes and the sample.

Chapter 9

Background

9.1 Contact resistivity

In solar cells, contact resistance can be an important loss mechanism, limiting cell efficiency. As a result, it is an important parameter to minimize. While the total contact resistance can be defined as $R_c = \frac{V}{I}$, with V and I being the voltage along the contact and the total current respectively, this changes with contact area. A more useful quantity is the contact resistivity, also known as specific contact resistance, which is area independent. This ρ_c is defined not using the total current, but the current density J:

$$\rho_c = \left.\frac{\partial V}{\partial J}\right|_{V=0}. \tag{9.1}$$

While from a theoretical point of view this description of contacts in terms of $J(V)$ sounds perfectly reasonable, its usage can be challenging in practice. To understand the problem, consider preparing a sample of area A and assuming that the current is uniformly distributed along the contact. The definition then easily translates to $\rho_c = \frac{V}{I}A$, where the total current I and induced voltage V can be measured. In reality, the current distribution into a contact can be localized near the edge of the contact, an effect called current crowding[5]. The current density decays exponentially with characteristic length $L_t = \sqrt{\frac{\rho_c}{R_\square}}$, called the transfer length, here $R_\square$ is the sheet resistance of the wafer. This phenomenon is illustrated in Figure 9.1.

This effect will be explained in more detail in Chapter 10, but first, let's think about its experimental implications. If the transfer length is much larger than the contacts, then the current will effectively be equally distributed. Sadly, for the samples used in this work, the transfer length

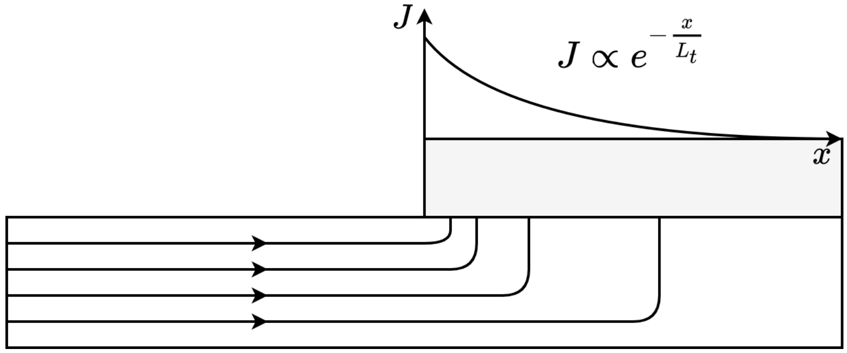

Figure 9.1: Illustration of current crowding along the edge of a contact. The current density J decays exponentially with distance from the contact edge. Shown are a wafer and a contact, current flows into the wafer from the left and into the contact, as indicated by the arrows.

was often found to be smaller than the contact dimensions. In such cases measuring V and J is not trivial, as they can vary greatly within the contact. In contrast to these locally defined V and J, it is typically only the total current, I, and *some* induced voltage, V_M, that can be measured experimentally. This is the main challenge of contact resistivity measurements: reliably distilling local $J(V)$ behaviour from global $I(V_M)$ measurements. In the next sections some typical solutions to this challenge will be discussed. Sadly, most of these methods involve patterning and etching, which, as discussed, can be difficult for ZnO:Al. TODO: does the next part fit here? Within the context of this project, symmetric lifetime samples were often made, consisting of a substrate with ZnO:Al deposited on both sides. These are further processed by thermal annealing after optional deposition of an Al_2O_3 capping layer. As this capped etching step is one of the focuses of this work, it is desirable to not change this process too much for contact resistivity samples. This is the main motivation for this part of this thesis, to figure out a way to quantify the contact resistivity of Si-ZnO:Al contacts using the available lifetime samples, without needing to drastically alter them.

9.2 Typical measurement methods

1. Cox and Strack In the Cox and Strack (C&S) method[6] samples are made that feature circular contacts of varying size on one side of the sample, while the other side has a full backplane contact, as illustrated

in Figure 9.2.

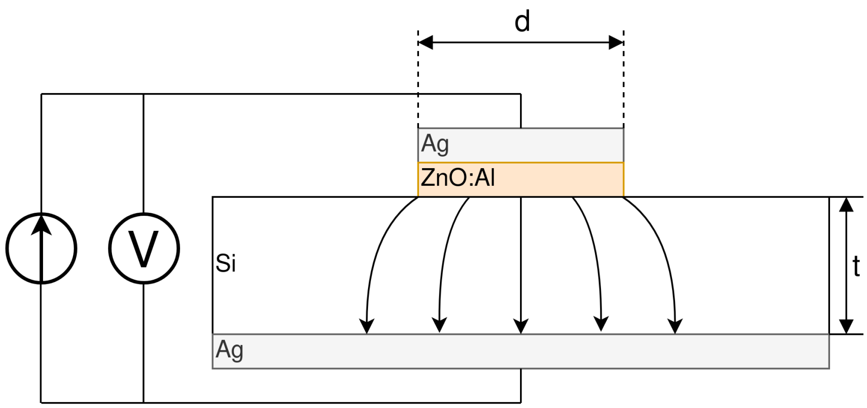

Figure 9.2: Illustration of a Cox and Strack measurement setup, the ZnO:Al and covering Ag layers are circularly shaped with diameter d, the Si and bottom Ag layers are much larger than the circular contact. t indicates the thickness of the Si layer. In practice, a single sample would be covered by multiple dots of varying diameter. The spreading resistance in the silicon scales differently with d than the contact resistance does, so that it can be fit out with sufficient data points.

The resistance between the backplane and the circular contacts is then measured for the different circular contacts. The main assumption here is that the total resistance can be described as a sum of three resistances: contact resistance R_c, spreading resistance R_s, and some fixed residual resistance R_0. Cox and Strack originally modeled these terms as

$$R_T \approx \underbrace{\frac{\rho_W}{\pi d} \arctan\left(\frac{4t}{d}\right)}_{R_s} + \underbrace{\frac{\rho_c}{\frac{1}{4}\pi d^2}}_{R_c} + R_0, \tag{9.2}$$

where d is the diameter of the contact, ρ_W is the wafer resistivity, ρ_c the contact resistivity and t is the thickness of the wafer [3]. Since the contact and spreading resistances depend differently on the contact radius, the contact resistivity can be determined by varying d and fitting to the model. While more accurate models for the resistance terms have been found [7, 2], the concept behind the measurement stays the same. The practical implications of this method are that samples have to be precisely made, the circular contacts are typically tens of micrometers in radius. TODO: source, this depends on resistances, how? To make structures like this one would need to remove part of the contacting layer, this extra processing, as explained previously, is best avoided. TODO: what measurement range?

2. Transfer length method The transfer length method (TLM) somewhat resembles the C&S method in the sense that multiple sample geometries are used to fit out the contact resistivity. In TLM, the chosen geometry can be either linear or circular TODO: cite, these variants are conceptually similar, so only the linear variant is discussed here. A linear TLM setup is illustrated in Figure 9.3.

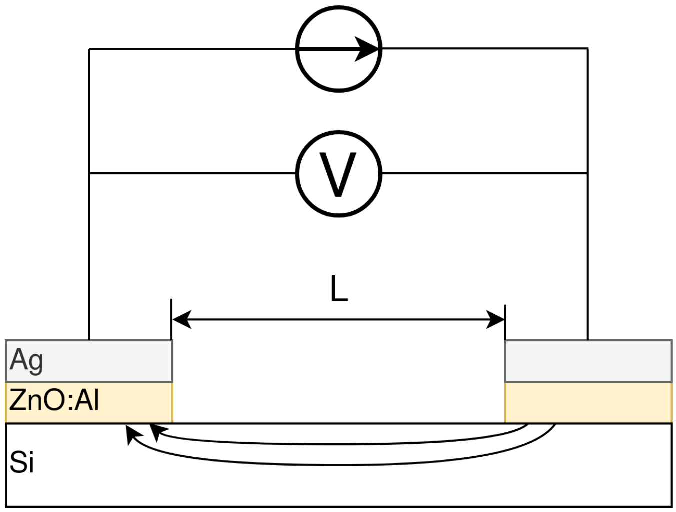

Figure 9.3: Side view illustration of a TLM measurement setup, on a rectangular sample of width W (not shown) several rectangular contacts are made, two shown here. The distance L between the contacts is varied. Note that the current is not uniformly distributed over the contact, but is localized within a transfer length L_t.

In this setup the total resistance consists of twice the contact resistance R_c and the resistance of the Si wafer R_w. The wafer resistance can be expressed as

$$R_w = \frac{LR_\square}{W}, \tag{9.3}$$

in which W is the width of the sample and $R_\square$ is the sheet resistance of the wafer.

Through current crowding, the currents are effectively localized to within a transfer length $L_t = \sqrt{\frac{\rho_c}{R_\square}}$ of the contact edge, this length will be derived in Chapter 10. This current crowding implies that the contact has an effective area of WL_t. Now take for the contact resistance $R_c = \frac{\rho_c}{WL_t} = \frac{R_\square L_t}{W}$, where the definition of L_t was used to obtain the second expression. Now the total resistance can be expressed as

$$R_T = 2\underbrace{\frac{R_\square L_t}{W}}_{R_c} + \underbrace{\frac{LR_\square}{W}}_{R_w} = \frac{R_\square}{W}(2L_t + L). \tag{9.4}$$

Here, the horizontal and vertical intercepts signify twice the transfer length and twice the contact resistance respectively, as shown in Figure 9.4.

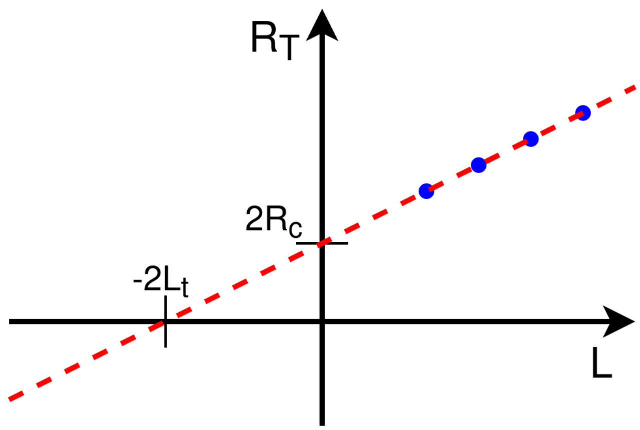

Figure 9.4: Example of a TLM analysis, the red fit line intercepts the horizontal axis at $-2L_t$ and the vertical axis at $2R_c$.

After finding the intercepts, the specific contact resistivity can be found as $\rho_c = R_c L_t W$ TODO: source.

The drawbacks of this method are similar to those of the C&S method, patterning and etching steps are required, making TLM not only difficult, but also possibly undermining the validity of the obtained results. Again, the ZnO:Al film should be partially removed in a controlled way, which is best avoided. A difference with the C&S method is that TLM samples imply symmetric measurements of a contact, in Ohmic contacts this is not an issue, but since in TLM the contacts are always in an antiseries configuration, this can make non-Ohmic contacts difficult to characterize.

3. Cross bridge Kelvin resistor While the previously described methods rely on being able to fit out the contact resistivity from some set of measurements, the cross bridge Kelvin resistor (CBKR) method takes a

different approach. In essence the method is a top-down four-terminal measurement, a current is driven from the top to the bottom of a sample using two terminals, while two other terminals are used to measure the resulting voltage.

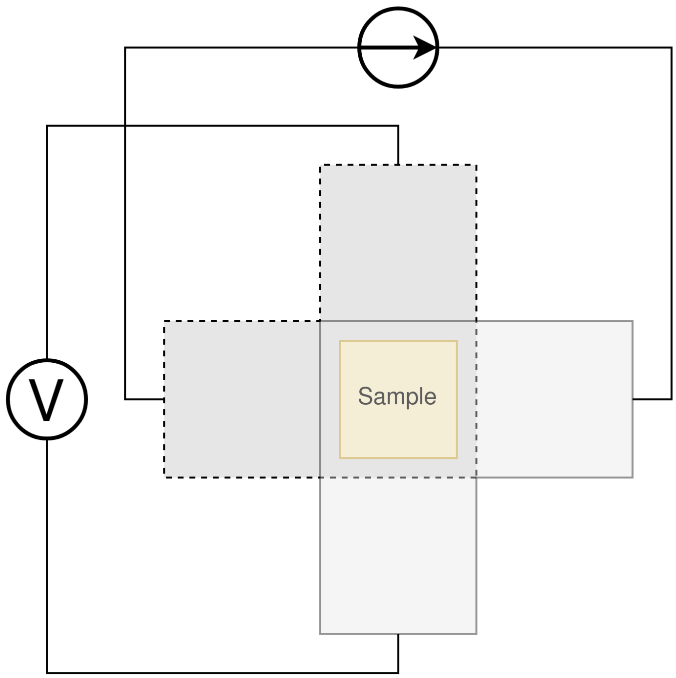

Figure 9.5: Illustration of a CBKR setup, shown are two L-shaped electrodes with a sample located in between. The electrodes are not in direct contact with each other. A current is driven from one of the legs of an L, through the sample, through the opposing leg of the other L. Meanwhile the resulting voltage is measured along the remaining legs. Also shown is a misalignment between the edges of the sample and the edges of the electrodes, this should ideally be small.

These electrodes are formed as two L-shapes, one on either side of the sample, with the “legs” opposed to each other. One set of opposed legs is used to drive the current, while the other opposed set is used to measure the voltage. With this approach parasitic resistances are easily ignored, as the voltage measuring wires carry no current.

Measure the total resistance of the sample, and multiply this by its area to get the *measured* specific resistance,

$$\rho_M \equiv \frac{V_{\text{meas}}}{I_{\text{src}}} A, \tag{9.5}$$

ideally this should equal the specific resistance, ρ_c, of the sample, but this relies on some assumptions that will be checked next.

One of there assumptions is that the current is evenly distributed over the sample, or equivalently, that the contacting electrodes form isopotentials. When measuring samples with low specific resistivities this might not hold, currents can be localized near the edge of the sample, and the measured voltage might not accurately represent the average voltage across the sample. Additionally, misaligned contacts can result in currents "wrapping around" the sample, this can result in an overestimation of the average voltage over the sample. TODO: illustrate wrap-around

This effect was modeled by Schreyer and Saraswat [4], defining the measured contact resistivity ρ_M as the product of measured resistance and sample area, and the transfer length L_t as $\sqrt{\frac{\rho_c}{R_\square}}$, their main result can be expressed as,

$$\frac{\rho_M}{\rho_c} = 1 + \underbrace{\frac{4}{3}\frac{\delta^2}{W_x W_y}\frac{A}{L_t^2}\left[1 + \frac{\delta}{2(W_x - \delta)}\right]}_{C_g}, \tag{9.6}$$

in which δ is the sample misalignment, and W_x and W_y are the thicknesses of the legs of the electrodes. Here the second term is referred to as the geometric correction factor, or C_g. Ideally C_g is small, so that $\rho_M \approx \rho_c$, this can be realized by using small samples, small misalignments, and highly conductive electrodes. Luckily C_g can easily be estimated.

TODO: how does next section fit here? Taking $\rho_c \approx 10\text{m}\Omega\text{cm}^2$ as a lower bound, and suppose using pieces of household aluminium foil for contacts ($R_\square \approx 3\text{m}\Omega_\square$, measured with a four-point probe), this gives a worst case (i.e. shortest) transfer length of around 2 cm. For easy measurements, the needed samples should not be much smaller than a squared cm, otherwise they will be difficult to cleave and handle with tweezers. By cutting the foil carefully, electrodes can be made with an estimated misalignment of around one mm. Substitution yields a C_g on the order of magnitude of a few thousandth's, indicating that geometric effects will not be significant in this setup.

In contrast to TLM and the C&S method, no patterning and etching steps are required by the CBKR method, making it a viable option for ZnO:Al samples. Still, there are some practical drawbacks to this method regarding the fabrication of test structures. In practice it can be difficult to cleave samples to specified dimensions, so that electrodes need to be custom made for each sample piece to reduce misalignment. Additionally, making sure that there are no shorts between the flimsy pieces of aluminium foil can be challenging. Experience shows that strategically placed pieces of insulating tape can help, but in the end eyebrows will probably be raised when reading “we sandwiched the sample between some household foil and duct tape, and it just appeared to work” in the methods section of any report. Despite these drawbacks, by working carefully it is possible to make these structures from aluminium foil. Due to its compatibility with the ZnO:Al samples, the CBKR method can be used as a good sanity check for any new measurements of these samples. TODO: measurement limits.

4. Pin to plate The challenges of measuring contact resistivities of ZnO:Al films were known at the start of this project, previous experience showed that reliable patterning and etching of this material is difficult, making TLM and the C&S method impractical. The approach that had been used to far was to clamp samples between a copper plate and some of the probe pins of the already available four point probe setup, as illustrated in Figure 9.6. One of the probe pins would be used to drive a current to the plate, while another pin would be used to measure the voltage across the sample. The copper plate would serve as both a current driving electrode and a reference voltage since, due to its high conductivity, the electric fields within the plate can be assumed to be negligible.

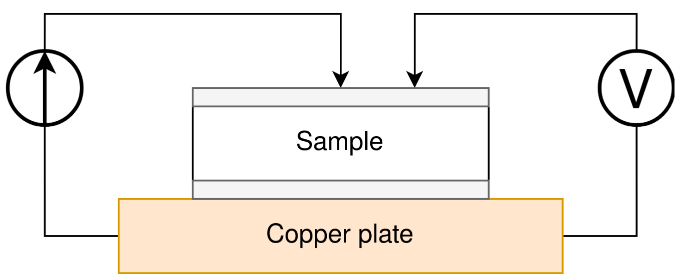

Figure 9.6: Illustration of a pin to plate measurement, featuring a copper base plate on which a silver coated sample is located. A current is driven between a pin and the base plate, while the voltage between another pin and the base plate is measured.

In essence this method is somewhat similar to the CBKR method, where a current is driven through the sample, *the* resulting voltage is measured, and the resulting resistance is multiplied by sample area to get the specific resistivity. While in the CBKR method the average voltage along the sample is measured (neglecting geometric resistance), in the pin to plate method the relation between measured voltage and average voltage is not so clear. Due to the contacting geometry, the voltage in the top contact is highly nonuniform, so that the measured voltage can differ by orders of magnitude on a single sample, depending on where this voltage is measured. These inhomogeneities will be analyzed in detail in Chapter 10.

It quickly became clear that this method provided neither reliable nor valid results, since measurements on exactly the same sample could yield values that vary by orders of magnitude. Nonetheless, the extreme ease of measurement compared to the previously discussed measurement methods made it an interesting candidate for further investigation. If the poorly chosen probing geometry is the cause of the problematic voltage nonuniformities, then maybe a different choice of probing geometry could solve this problem.

Addressing these challenges in the pin to plate method is the goal of the rest of this thesis. The first step is to better understand the nature of current (or equivalently, voltage, by Ohm's law) inhomogeneities, this will be the goal of Chapter 10.

Chapter 10

Theory

10.1 Transfer length effects

So far, all the top-down measurement methods had to mitigate one phenomenon, transfer length effects. Consider ideal conductors used as contacts, as these form regions of equal electric potential, the potential difference between top and bottom of the sample will be equal everywhere. The driven current density will be uniform, found simply by: $J = \frac{\Delta V}{\rho_s}$. In this idealized case, contact resistivities would be trivial to measure, but in reality the driven current distributions and potential differences can be significantly inhomogeneous, as illustrated in Figure 10.1.

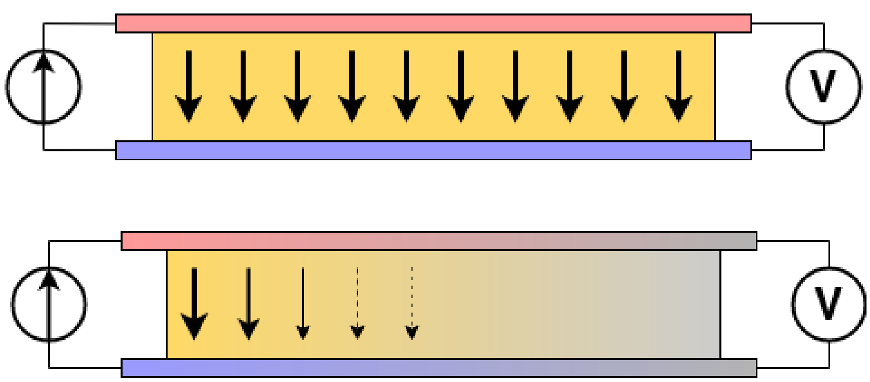

Figure 10.1: A comparison between contacting with ideally conducting electrodes (top) and electrodes with significant resistivity (bottom). Positive and negative voltages are shown as shades of red and blue in the electrodes, while the current density through the sample is depicted using arrows and shades of yellow. In the ideal case the contact voltages and current densities are uniform, while in the non-ideal case the current distribution is localized near the current injection point of the contacting electrodes.

To quantify these effects, the interaction between electrodes and sample was modeled, as illustrated in Figure 10.2.

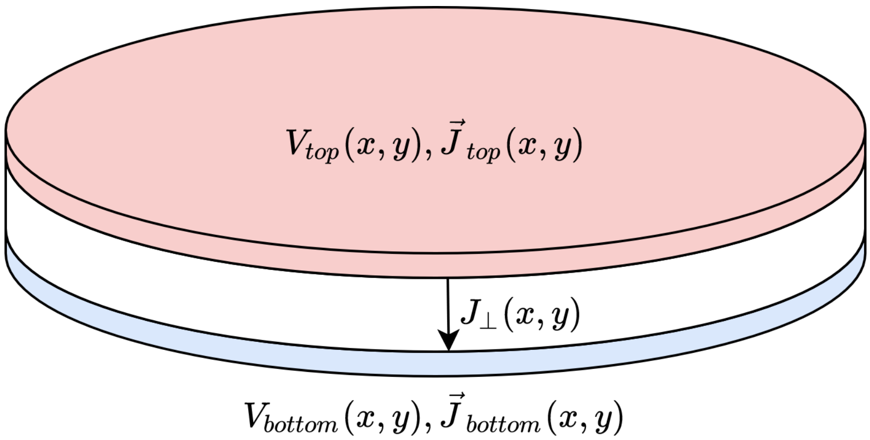

Figure 10.2: A model of a sample with two contacting electrodes. In the electrodes the current density is determined from the electrodes' conductivity and the electric fields. The current density through the sample can be determined from the stack resistivity ρ and the local potential difference between the top and bottom electrode.

1. Governing equations In this model an arbitrary slab of sample and electrodes is considered, oriented along the x-y plane, with the z-direction defining the top and bottom of the setup. The electrodes are considered to be very thin, and relatively conductive, so that the voltage within each electrode is independent of z. Within these electrodes, the current density is determined by Ohm's law, so that

$$\vec{J}_{top} = -\sigma \nabla_{(x,y)} V_{top}(x, y), \tag{10.1}$$

and

$$\vec{J}_{bottom} = -\sigma \nabla_{(x,y)} V_{bottom}(x, y), \tag{10.2}$$

in which σ is the conductivity of the electrode material. The current density through the sample is given by

$$J_{\perp} = \frac{V_{top} - V_{bottom}}{\rho}, \tag{10.3}$$

for some specific sample resistance ρ. Consider charge conservation in any region Ω in the top electrode, which can be expressed as a sum of currents flowing into the region from other parts of the electrodes, and a current flowing into the sample:

$$0 = \int_\Omega \vec{J} \cdot \mathrm{d}\vec{A} = \int_\Omega J_\perp \mathrm{d}A + \oint_{\partial\Omega} \vec{J}_{top} \cdot \hat{n} h \mathrm{d}s, \tag{10.4}$$

where h is the thickness of the electrode. Substitution of the current densities followed by application of the divergence theorem yields

$$0 = \int_\Omega \frac{1}{\rho}(V_{top} - V_{bottom})\mathrm{d}A - \int_\Omega \sigma h \nabla^2_{(x,y)} V_{top} \mathrm{d}A, \tag{10.5}$$

and similarly for the bottom equation, except the sign of the $J_\perp$ contribution is switched

$$0 = \int_\Omega \frac{1}{\rho}(V_{top} - V_{bottom})\mathrm{d}A + \int_\Omega \sigma h \nabla^2_{(x,y)} V_{bottom} \mathrm{d}A. \tag{10.6}$$

Adding the two together, and letting $\phi \equiv V_{top} - V_{bottom}$, one gets

$$0 = \int_\Omega -\sigma h \nabla^2_{(x,y)} \phi + \frac{\phi}{\rho} \mathrm{d}A \tag{10.7}$$

As the choice of Ω was arbitrary, the integrand must vanish almost everywhere, so that

$$\nabla^2 \phi = \frac{1}{\sigma h \rho} \phi = \frac{R_\square}{\rho} \phi, \tag{10.8}$$

where $\frac{1}{\sigma h}$ is recognized as the sheet resistance $R_\square$.

No PDE is complete without appropriate boundary conditions, in this work Neumann boundary conditions are considered, as these describe four-point probing setups the best: a current distribution is driven along some part of the domain boundary, and some resulting potential difference is measured. In dimensionless form, the equation can be written as

$$\tilde{\nabla}^2 \phi = \left(\frac{L}{L_t}\right)^2 \phi \equiv k^2 \phi, \tag{10.9}$$

where L is the characteristic dimension of the sample, and $L_t \equiv \sqrt{\frac{\rho}{R_{sq}}}$ is the familiar transfer length, and the dimensionless Laplacian is given by $\tilde{\nabla}^2 = \frac{1}{L^2} \nabla^2$. In following sections the tilde on the Laplacian will be omitted, so that the dimensionless form of the PDE is given by

$$\nabla^2 \phi = k^2 \phi, \qquad \text{Contact} \tag{10.10}$$

$$\nabla \phi \cdot \hat{n} = f \qquad \text{Contact edge.} \tag{10.11}$$

2. Uniqueness of solutions To show that solutions are unique, consider two solutions, ϕ_1 and ϕ_2 and let $\hat{\phi} \equiv \phi_1 - \phi_2$, the goal will be to show that the PDE and boundary conditions force ϕ to vanish. Linearity shows that $\hat{\phi}$ must obey

$$\nabla^2 \hat{\phi} = k^2 \hat{\phi}, \quad \Omega \tag{10.12}$$

$$\nabla \hat{\phi} \cdot \hat{n} = 0 \quad \partial\Omega. \tag{10.13}$$

Now consider the following integral,

$$\int_\Omega \nabla \cdot (\hat{\phi} \nabla \hat{\phi}) \mathrm{d}x = \oint_{\partial\Omega} \hat{\phi} \nabla \hat{\phi} \cdot \mathrm{d}\vec{A} \overset{\text{B.C.}}{=} 0, \tag{10.14}$$

apply the chain rule

$$0 = \int_\Omega \nabla \cdot (\hat{\phi} \nabla \hat{\phi}) \mathrm{d}x = \int_\Omega \hat{\phi} \nabla^2 \hat{\phi} + \nabla \hat{\phi} \cdot \nabla \hat{\phi} \mathrm{d}x, \tag{10.15}$$

and apply the PDE to clear the $\nabla^2 \hat{\phi}$ term,

$$0 = \int_\Omega k^2 \hat{\phi}^2 + \left| \nabla \hat{\phi} \right|^2 \mathrm{d}x. \tag{10.16}$$

With the inner product

$$\langle \phi, \psi \rangle \equiv \int_\Omega k \phi \psi + \nabla \phi \cdot \nabla \psi \mathrm{d}x, \tag{10.17}$$

Equation 10.16 can be recognized as $\langle \hat{\phi}, \hat{\phi} \rangle = 0$, so that $V_{top} - V_{bottom} \equiv \phi = 0$, proving that solutions of Equations 10.10 and 10.11 are indeed unique.

3. Influence of transfer length Now, let's apply this model to a few practical situations, starting with a pin to plate measurement. For simplicity, the samples are modeled as circular with radius 1, excluding the origin. Through an appropriate choice of k the solutions can describe any arbitrary combination of sample radius, contact resistivity and sheet resistance. As all currents are contained in the sample, the current density must vanish at the boundary, so that $\phi'(1) = 0$. The origin is excluded from the domain, so that a current source can be located here. In experimental conditions the total supplied current, I, is known. In this model however the average potential drop, $\bar{\phi}$, is specified, so that

$$\bar{\phi} = \frac{\int_\Omega \phi \mathrm{d}A}{\int_\Omega \mathrm{d}A} = \frac{2\pi}{\pi R^2} \int_0^1 r\phi(r) \mathrm{d}r = 2 \int_0^1 r\phi(r) \mathrm{d}r. \tag{10.18}$$

Since we're interested in deviations from the average potential, the average potential is fixed at a dimensionless value of 1. In the adopted cylindrical coordinates, the PDE can be expressed as

$$r^2\phi''(r) + r\phi'(r) - r^2k^2\phi(r) = 0, \tag{10.19}$$

which is known as the modified Bessel equation. This modified Bessel function has solutions:

$$\phi(r) = AI_0(kr) + BK_0(kr), \tag{10.20}$$

in which A and B are integration constants and I_0 and K_0 are modified Bessel functions of the first and second kind [1]. By applying the boundary and integral conditions the integration constants can be found. These steps are omitted here, as it is mostly textbook linear algebra. In a simpler 1D cartesian system, the PDE reduces to $\phi'' = k^2\phi$, which was solved with a similar boundary and integral condition. The solutions for both geometries and varying k are shown in Figure 10.3.

Figure 10.3 clearly shows the impact of the transfer length on the homogeneity of the current distribution, short transfer lengths (compared to sample dimensions) result in very inhomogeneous current distributions. Additionally, when compared at similar transfer lengths, the cylindrical solutions are much less homogeneous than the cartesian ones.

10.2 Idea: reduce effective sample dimensions

Suppose you were to conduct a four-point probing experiment in either geometry, in which a current is driven through the sample, and some potential difference between the top and bottom of the sample, ϕ_M, is measured. What would be a good way to perform these measurements?

To answer this question, it is useful to first estimate L_t for the samples of interest. As the current distribution is least homogeneous for small L_t, it is safest to underestimate it by using large sheet resistivities and low stack resistivities. While the stack resistivity is of course not known before the measurements, the lowest order of magnitude of ρ was estimated at 10 mΩcm^2, while for the used AZO films, $R_{sq} \approx 100\ \Omega$ is not uncommon, in this case the transfer length is on the order of 0.1 mm. QUESTION: is meer toelichting nodig?

In practice, we'd like to be able to work with samples with dimensions of at least a few mm, not just because these are easier to handle, but because

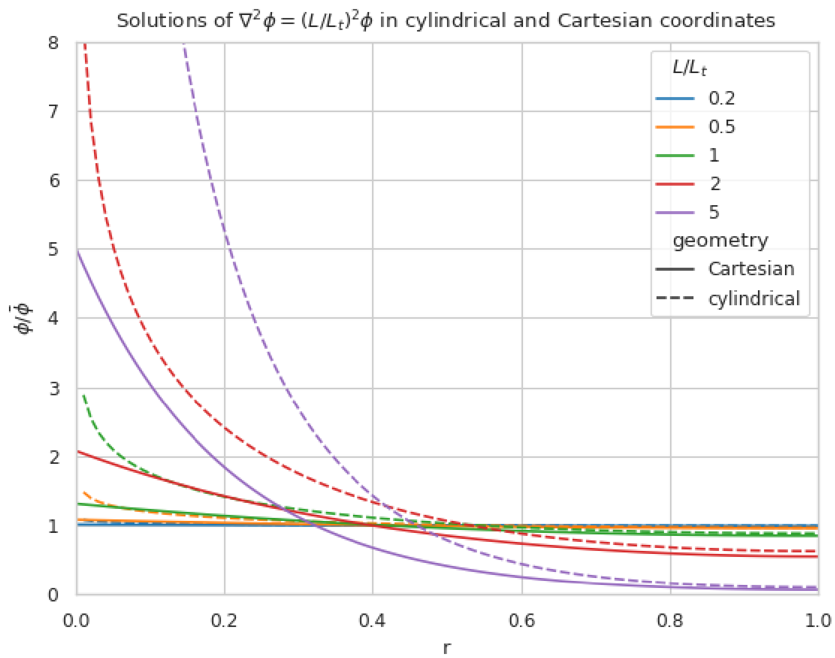

Figure 10.3: A comparison of solutions for ϕ on $(0,1]$ in Cartesian and cylindrical coordinates, for varying $k \equiv \frac{L}{L_t}$. With boundary condition $\phi'(1) = 0$ and integral condition $\bar{\phi} = 1$. Note that the cylindrical solutions have much steeper gradients than the Cartesian ones, and that the homogeneity of the current distribution depends strongly on k, with large k leading to very inhomogeneous currents. TODO: capitalize cylindrical

these can be easily be prepared by hand-cleaving a bigger sample piece. In these cases k would be significantly larger than 1, so the majority of current will be driven only through a small part of the sample near the current drive electrode.

The goal now is to reduce k through some means, in the ideal limiting case $k = 0$, but how close is close enough? In Figure 10.4, the normalized (with respect to the average) value of ϕ is shown at the extremes of a sample for different k, the black horizontal line indicates 99%. This shows that, in order to measure the average potential to within a percent relative error, k has to be around 0.25 or lower.

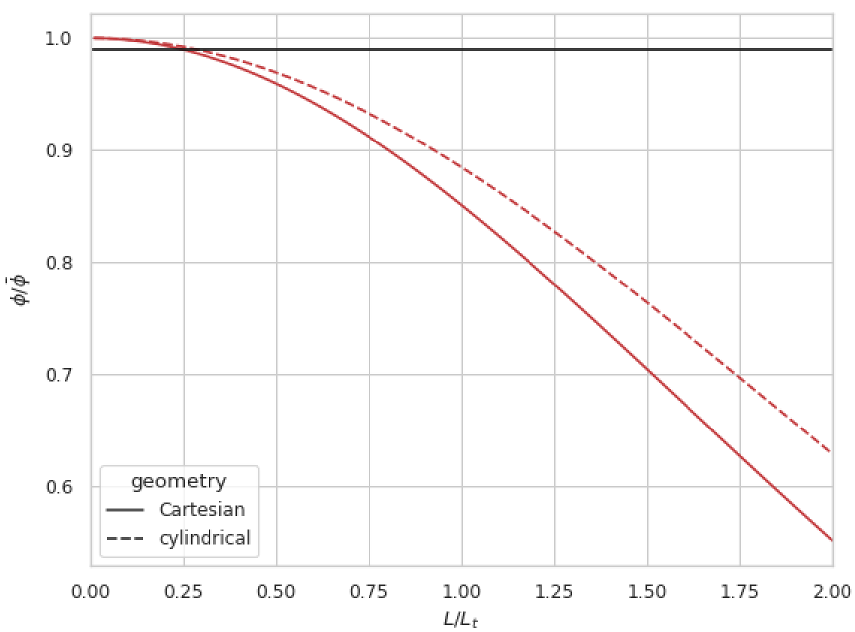

Figure 10.4: $\frac{\phi_M}{\bar{\phi}}$ at the edge of the sample, as function of $\frac{L}{L_t}$. For small $\frac{L}{L_t}$ the potential measured at the edge very closely resembles the average potential.

To realize this goal of decreasing $\frac{L}{L_t}$, two separate approaches are combined. The first is to increase L_t by making the contacting layers more conductive, this is achieved by depositing 300 nm of silver by e-beam evaporation. This increases L_t to approximately a few millimeters. QUESTION: meer toelichting nodig?

The second approach is to effectively reduce L by controlling the probe geometry. At first glance, L appears to be determined by the sample size, a current is driven through some point, and this current cannot flow out of the sample, represented in the boundary condition $\phi'(L) = 0$. An obvious option to reduce L could be to simply cut smaller samples, but in the millimeter range this is difficult, especially when areas need to be accurately determined. Working with tiny samples, while perfectly fine in theory, is undesired in practice, so can we decrease L in bigger samples? The answer is yes! The trick lies in the nature of the boundary condition, it is only required that $\phi'(L) = 0$, but does this imply that the sample is contained in the $0 < x < L$ range? Not neccesarily. As an example, consider the one dimensional case: $\phi''(x) = k^2\phi(x)$ on $(0, 1)$. Now instead of applying a zero flux condition at any domain edge, simply consider solutions that are symmetric around $x = \frac{1}{2}$. These can easily be constructed from the solutions, $\phi_k(x)$, as

$$\phi_{k,\mathrm{sym}}(x) = \frac{1}{2}(\phi_k(x) + \phi_k(1 - x)). \tag{10.21}$$

These solutions correspond to a current being injected through two separate contacts, located at $x = 0$ and $x = 1$.

Symmetric solutions are shown in Figure 10.5, it is clear that now $\phi'(\frac{1}{2}) = 0$. Notice the similarity between the solutions as shown in Figure 10.3 and the left half of Figure 10.5, they are the same! Apparently driving currents with a grid of symmetric electrodes will let us effectively change L.

QUESTION: is dit argument duidelijk?

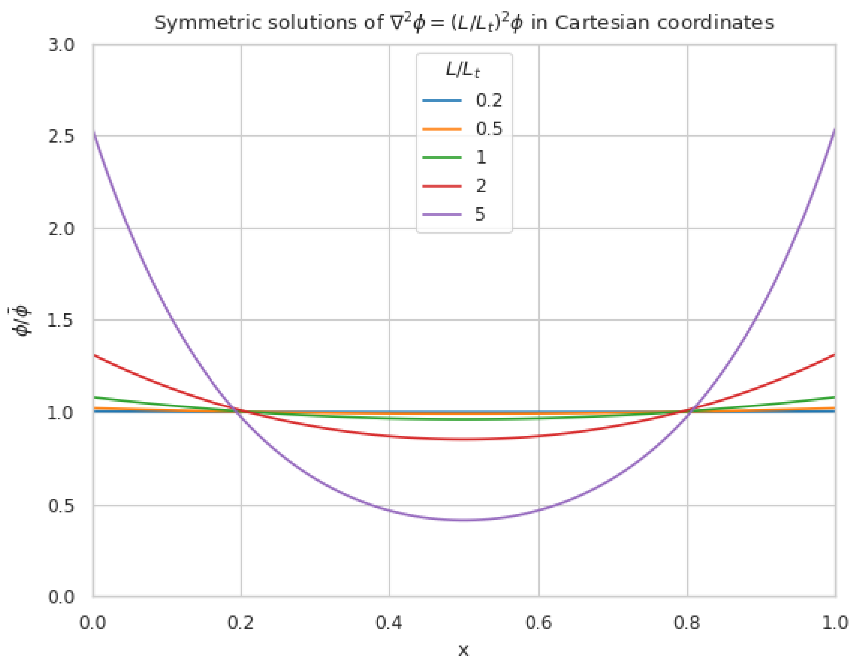

Figure 10.5: Symmetric solutions to Equation 10.10 in a 1D Cartesian geometry. Note that $\phi' = 0$ halfway between the two contacts, in this case the boundary conditions are imposed through the contact spacing, not through the total dimensions of the sample.

Chapter 11

New approach

This approach was realized using custom made printed circuit boards (PCBs), as shown in Figure 11.1. The PCBs feature a pad of regularly spaced copper lines, covering an area of 15 by 15 mm^2. The copper lines are alternately connected to either of the shown pins, so that they resemble interleaved combs. To perform a measurement, a sample is clamped between two such PCBs, and a current is driven between two combs on alternate sides of the sample, while the other combs are used to measure the resulting potential across the sample in a four-terminal configuration. The used copper lines were 0.6 mm wide and spaced 0.3 mm apart, with this spacing and a sample spreading length on the order of half a cm, the requirement that $\frac{L}{L_t} < 0.25$ is easily met, so that the current distribution can be considered homogeneous.

Practically, the measurements come down to the following steps:

1. Create samples that:
    - Have a spreading length significantly larger than the distance between the fingers of the PCBs to be used. Cover with silver if neccesary.
    - Are homogeneous, this might not be the case when deposited films wrap around the samples.
    - Feature no edge deposited conductive films, it is recommended to cleave off the edges of the samples after silver deposition.
    - Have an accurately known surface area, A, in this work this was achieved with a computer vision method, which will be discussed later. TODO: describe script in appendix
    - Fit on the 15 mm by 15 mm measurement pads of the PCBs.
2. Set up the resistance measurement system:
    - Use a sourcemeter in a four-terminal sensing configuration, in this work a Keithley 2400 was used.
    - Connect the current source terminals of the sourcemeter to "combs" on the two separate PCBs.
    - Connect the voltage measurement terminals to the remaining combs.
3. Clamp the sample between the PCBs
    - Make sure that the sample is located on the pads, and does not shift before measuring.
    - Use the alignment holes of the PCBs for consistent alignment.
    - Apply an evenly distributed pressure to the sample, this can be achieved with a glue clamp.
4. Perform a standard four-terminal resistance measurement, yielding resistance R.
5. Calculate the specific resistivity $\rho_s = R \cdot A$.

TODO: include figure of wiring

The interpretation of the measured stack resistivity depends on the used samples, as in this work symmetric samples were used, the stack resistivity must be larger than twice the interfacial resistivity of the AZO-Si interface. In this case an upper bound on contact resistivity can be given as $\rho_c < \frac{1}{2}\rho_s$.

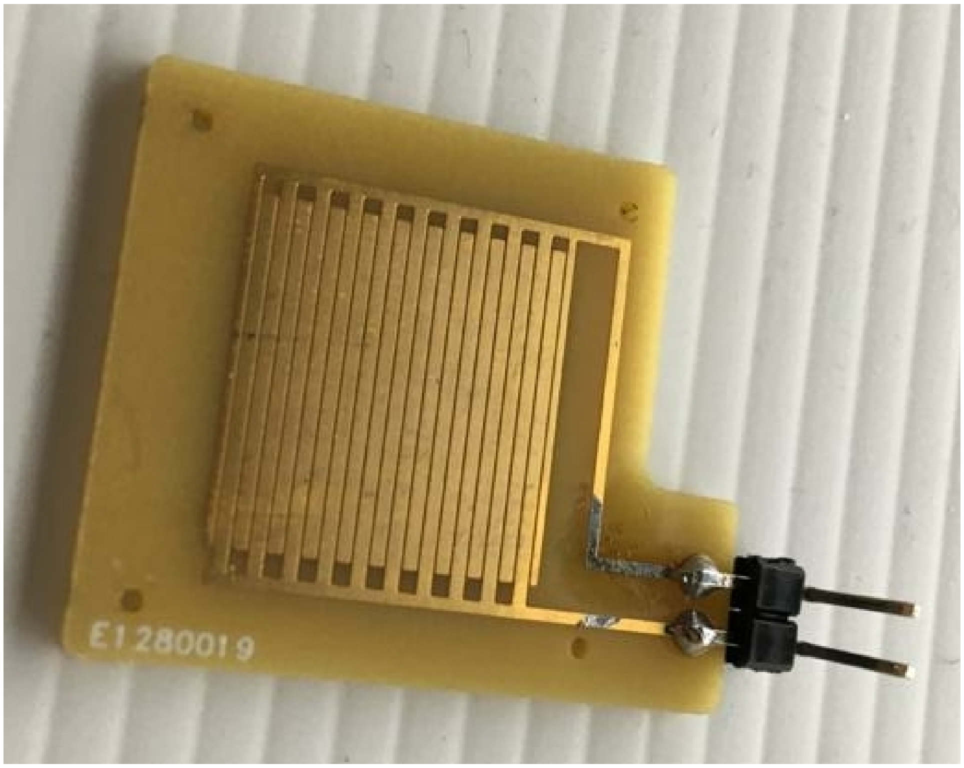

Figure 11.1: An image of a used PCB, shown are two interleaved comb-shaped copper contacts, these can be connected to measurement equipment using the two header pins. The four holes can be used to systematically align two PCBs using a pin.

Chapter 12

Characterization of measurement method

So far the case for PCB measurements has boiled down on purely theoretical arguments, in the following chapters the measurement method will be experimentally characterized. The characterization will focus on two desired properties of the new measurement: reliability and validity. A measurement method is reliable when it is reproducible, yielding the same results on each measurement. Reliability by itself is not enough though, simply because observations being close to each other does not imply that they are close to the *correct* value. A measurement is called valid if its results actually resemble what is **intended** to be measured. For a good measurement system these two qualities obviously go hand in hand.

While the reliability often refers to repeated measurements under the exact same conditions, this strict definition is not very useful when considering the PCB measurements, as the goal is to reliably measure the contact resistivity **without** regard to some sample handling details. For context, the initial measurement system (TODO footnote: detail pin to plate) proved quite reliable when a single sample was contacted and stayed fixed between measurements. Problems started appearing however, as soon as this sample was contacted with different pins, in slightly different locations, rotated a bit, or a different sample piece was used. The estimated contact resistivities varied unpredictably when even slight, to the user practically unnoticeable, changes were made to the setup. The goal here is not to be reliable under strict control of all influencing factors, but to be reliable in a somewhat chaotic environment, one in which the user can choose not to care about the exact shape and contacting points of their samples, and still get *reliable* results. For this reason, the term reliability is used in a looser sense in this work: a measurement is considered reliable when it yields similar (enough) results in a range of realistic usage scenarios.

More practically speaking, these “realistic usage scenarios” should at least include different contacting conditions, like where the sample is located and in which orientation, but also simply using another sample of differing dimensions. These reliability experiments were done by varying exactly the mentioned conditions and measuring if these influence the measurement, this will be discussed in more detail in following sections.

To check the validity of the measurement, a reference measurement is needed. Ideally a sample with a well known specific resistance could be used, but these were not available. Another option is to take a sample, measure the specific resistance through some other means, and then compare the results with the new method. This concurrent validity test was chosen, in which the novel method was compared to a cross bridge kelvin resistor (CBKR). The choice for a CBKR test was made since it can handle the same type of samples that the PCBs can. The needed patterning for Cox & Strack and other methods would imply the need to make separate samples, process them differently, and just hope that they have the same specific resistance. A CBKR allows for measurements on the exact same samples as on the PCBs, without any alterations, making it fit for a direct comparison of measurement methods. The used CBKR setup will be discussed in more detail in Section 13.2.

Chapter 13

Results

13.1 Reliability

Ideally the PCB method should yield the same contact resistivities, regardless of

- Sample orientation,
- Sample position,
- Sample shape.

These assumptions were checked, starting with the sample orientation. Here the contact resistivity was measured for two cases, in the "long" case the long edge of the sample was aligned parallel to the fingers of the PCBs, while in the "short" case the short edge was aligned parallel to the fingers. This was done for two symmetric samples:

1. pSi substrate with r48 AZO annealed at 400C, measuring approx 4.5 mm by 6.5 mm.
2. 130 Ω n+ Si with r48 AZO annealed at 400C, measuring approx 6.5 mm by 9.0 mm.

The results are shown in Figure 13.1. For the pSi sample, the results are quite consistent, while for the n+ Si sample there is more spreading in the measurements. This can be explained by the pSi sample having a larger contact resistivity than the n+ Si sample, and thus a larger spreading length, this sample also happened to have smaller dimensions, so that overall the current distribution can be expected to be more homogeneous. Overall, the measurement seems most repeatable in the "short" configuration.

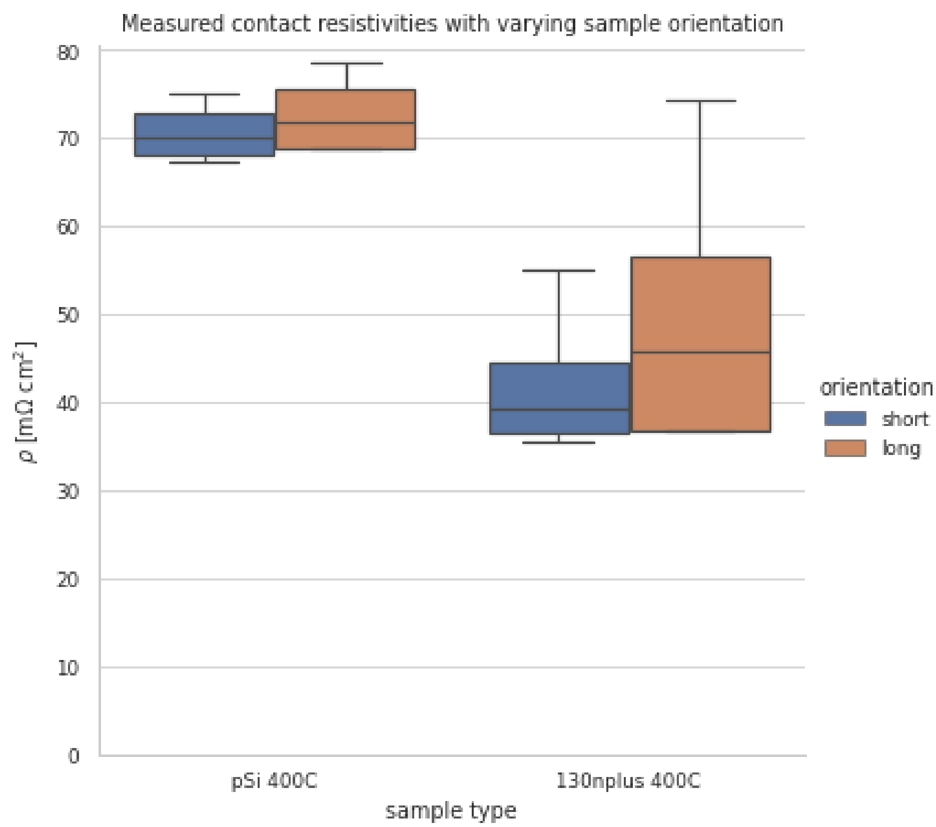

Figure 13.1: Measured contact resistivities with varying orientation. Two different samples were used, for which the contact resistivity was measured in different orientations. In the "short" cases, when the short side of the sample lies parallel to the PCB's fingers, the measurements are most reliable.

Next the location of the sample on the PCB was varied for a few samples. The samples were located at all four extreme corners of the PCB pad and at the center. Figure 13.2 shows the measured results for each of the tested samples, note the logarithmic vertical axis. This shows that the measurement is typically reliable on a per-sample basis. There are some clear deviations between pieces cut out of the same wafer, while these should all have the same contact resistivities, Figure 13.2 shows that this is not the case. A possible cause for this is backside deposition of Al_2O_3 resulting in nonuniform samples, which was observed to occur by TEM. TODO: reference to figure

TODO: how does this influence ρ_c, why is it expected to increase?

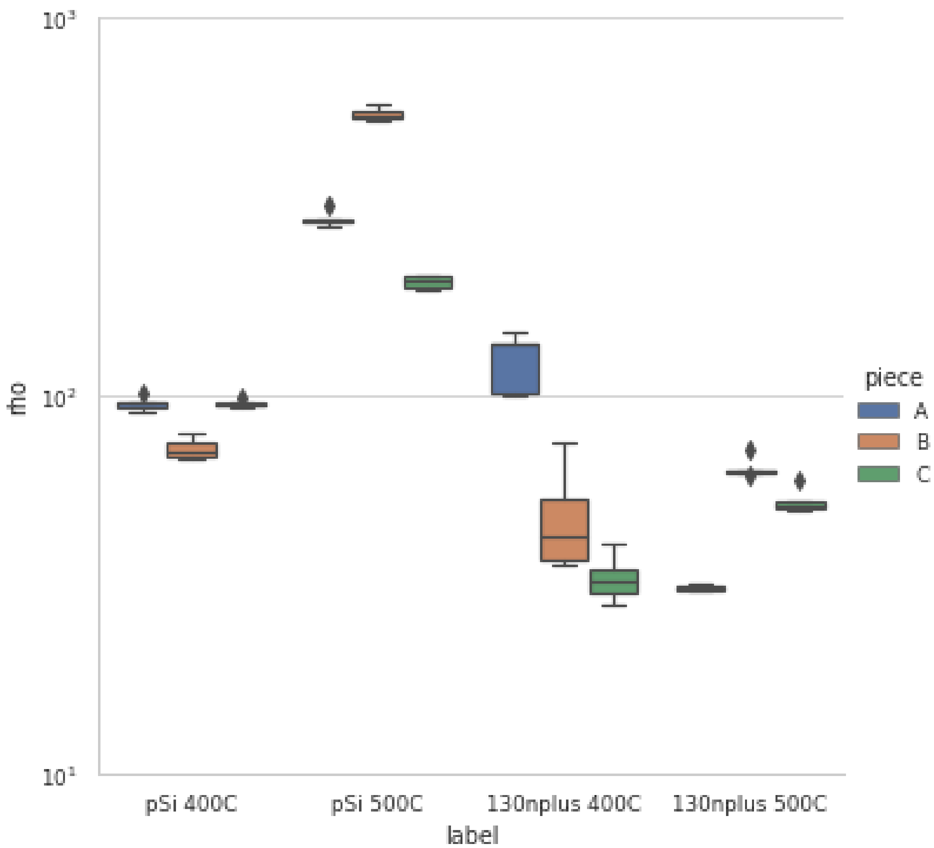

Figure 13.2: Measured contact resistivities of different pieces of different samples, the spread between measurements on different pieces are often larger than the spread within the pieces. The pieces are labeled in order of their overall size, A being the largest within each category.

13.2 Validity: Cross Bridge Kelvin Resistor comparison

Finally the PCB method was cross-validated with a Cross Bridge Kelvin Resistor (CBKR) setup which was carefully crafted from pieces of aluminium foil. While this alternate method is difficult and time consuming to perform, it provides a good sanity check for the PCB method. To do this, two L-shaped pieces of aluminium foil were cut, with the widths of the legs matching the dimensions of the samples. These contacting pads were made for each specific sample. Then the sample was clamped between the pieces of foil, while pieces of insulating tape ensured that no shorts could occur between the contacting pads. Two opposing "legs" were used to drive a current, while the potential difference was measured between the others, again in a four-point probe configuration. Several samples were used, for which the contact resistivity was measured multiple times with the PCB method and the CBKR method, Figure 13.3 shows that the results correlate strongly, here the error bars show the minimal and maximal values for each measurement.

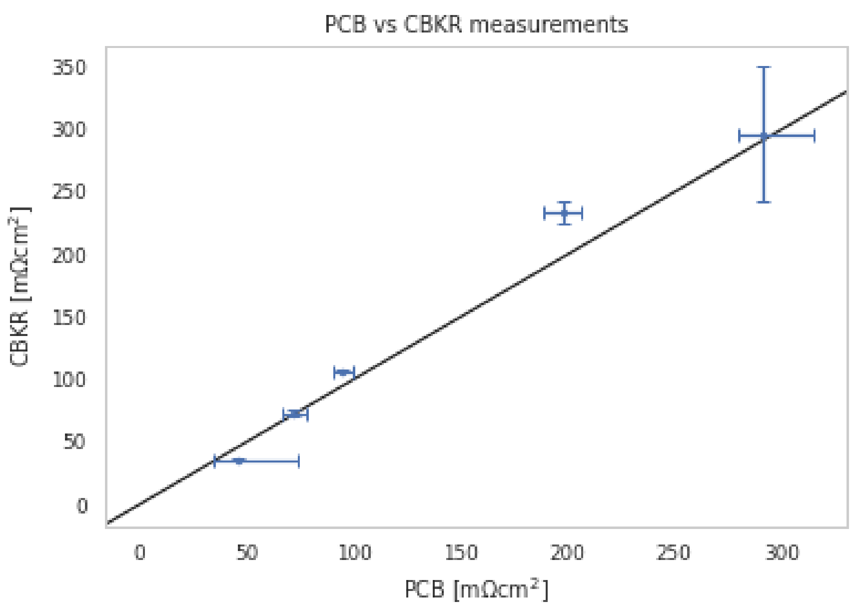

Figure 13.3: Comparison between PCB measurements and and CBKR measurements on a set of samples, the error bars indicate the minimum and maximum of the measured values. Ideally the measurements should match exactly, which is indicated by the black line.

Chapter 14

Conclusion

A method for easy contact resistivity measurements on laterally uniform samples was developed. This was achieved by contacting samples with custom made printed circuit boards, featuring interleaved comb-like copper contacts, which are used to drive a uniform current distribution through a sample. In contrast to the Cox & Strack and transmission line methods, which involve delicate sample patterning steps, the method developed here only requires uniform conductive contacting layers. This is especially important for ZnO:Al samples, since controlled etching of these layers is known to be difficult, rendering TLM and the C&S method impractical. In essence, the new method shows similarities to the CBKR method, both methods use a four terminal approach, and both aim to eliminate inhomogeneous currents by electrode design. In contrast to the CBKR method, in which the electrode dimensions need to match the sample dimensions, the PCBs used in the new method enable a rapid reuse of the same testing structure for samples of different dimensions.

Bibliography

[1] M. Abramowitz and I. A. Stegun. *Handbook of Mathematical Functions with Formulas, Graphs, and Mathematical Tables*. Dover, New York, ninth dover printing, tenth gpo printing edition, 1964.

[2] M. Ahmad, T. Ganguli, S. Patil, S. Major, Y. G. K. Patro, and B. M. Arora. Determination of contact resistivity by a modified Cox and Strack method in case of finite metal sheet resistance. *Solid-State Electronics*, 38(8):1437–1440, Aug. 1995.

[3] R. H. Cox and H. Strack. Ohmic contacts for GaAs devices. *Solid-State Electronics*, 10(12):1213–1218, Dec. 1967.

[4] T. Schreyer and K. Saraswat. A two-dimensional analytical model of the cross-bridge Kelvin resistor. *IEEE Electron Device Letters*, 7(12):661–663, Dec. 1986.

[5] D. Schroder and D. Meier. Solar cell contact resistance—A review. *Electron Devices, IEEE Transactions on*, 31:637–647, June 1984.

[6] D. K. Schroder. *Semiconductor Material and Device Characterization*. John Wiley & Sons, Inc., Hoboken, NJ, USA, Apr. 2005.

[7] M. van Rijnbach, R. J. E. Hueting, M. Stodolny, G. Janssen, J. Melskens, and J. Schmitz. On the Accuracy of the Cox–Strack Equation and Method for Contact Resistivity Determination. *IEEE Transactions on Electron Devices*, 67(4):1757–1763, Apr. 2020.

[8] P. Wuerfel. Physics of solar cells: From principles to new concepts. *Physics of Solar Cells: From Principles to New Concepts, by Peter Würfel, pp. 198. ISBN 3-527-40428-7. Wiley-VCH , March 2005.*, Mar. 2005.